Toward a Predictive Understanding of Slow Methyl Group Dynamics in Proteins

Dong Long,[†] Da-Wei Li,[†] Korvin F. A. Walter,[‡] Christian Griesinger,[‡] and Rafael Brüschweiler[†*]
[†]Department of Chemistry and Biochemistry, and National High Magnetic Field Laboratory, Florida State University, Tallahassee, Florida; and
[‡]Department of NMR-Based Structural Biology, Max-Planck Institute for Biophysical Chemistry, Göttingen, Germany

ABSTRACT The development of the most recent generation of molecular mechanics force fields promises an increasingly predictive understanding of the protein dynamics-function relationship. Based on extensive validation against various types of experimental data, the AMBER force field ff99SB was benchmarked in recent years as a favorable force field for protein simulations. Recent improvements of the side chain and backbone potentials, made by different groups, led to the ff99SB-ILDN and ff99SBnmr1 force fields, respectively. The combination of these potentials into a unified force field, termed ff99SBnmr1-ILDN, was used in this study to perform a microsecond time scale molecular dynamics simulation of free ubiquitin in explicit solvent for validation against an extensive set of experimental NMR methyl group residual dipolar couplings. Our results show a high level of consistency between the experimental data and the values predicted from the molecular dynamics trajectory reflecting a systematically improved performance of ff99SBnmr1-ILDN over the original ff99SB force field. Moreover, the unconstrained ff99SBnmr1-ILDN MD ensemble achieves a similar level of agreement as the recently introduced EROS ensemble, which was constructed based on a large body of NMR data as constraints, including the methyl residual dipolar couplings. This suggests that ff99SBnmr1-ILDN provides a high-quality representation of the motions of methyl-bearing protein side chains, which are sensitive probes of protein-protein and protein-ligand interactions.

INTRODUCTION

Conformational dynamics of biomacromolecules is critically important for their physiological function (1,2). Its characterization has therefore become a major focus of contemporary biophysics. Currently, the majority of protein dynamics studies have focused on the main chain. However, understanding the motions of side chains is of great interest, because the side chains of amino acids provide each amino acid its individual character and play an active role in protein behavior, including stability (3), folding (4), and molecular recognition (5,6). Technically, quantitative characterization of protein side chains by NMR is more challenging than for the backbone, due to spectral linewidths and overlaps. Nevertheless, methyl- and NH_3^+-amino-bearing side chains represent a notable exception, because the rapid rotation of methyl and amino groups about their symmetry axis significantly narrows the linewidths, making them amenable to quantitative studies for a wide range of systems (7–10). Methyl groups are often used as dynamical proxies of other side chains and as an indirect measure of local disorder (11).

Although NMR methodologies for measuring side-chain motions have substantially advanced during the past decade, a realistic description of the potentially complicated atomic trajectories by experiment alone with full spatial and temporal resolution has remained a formidable task. Therefore, all-atom molecular dynamics (MD) simulations represent a promising tool to significantly enhance the NMR-derived information. Yet, the success of this approach critically depends on the accuracy of the underlying force fields, which can be directly assessed by comparing with experimental NMR data. The AMBER ff99SB force field (12) has been benchmarked in recent years as a favorable force field for protein simulations (13–18). However, there is still considerable room for further improvement. Recently, the optimization of the backbone potentials of ff99SB based on a large set of experimental NMR chemical shifts was performed, and the resulting force field ff99SBnmr1 shows an overall improvement over ff99SB (19). Moreover, the side-chain dihedral potentials of four amino acids (ILDN), which recently have been reparameterized based on quantum mechanical calculations (20), show improved performance for side-chain motions. Due to the independent nature of these refinements focusing either on backbone (19) or side-chain torsion potentials (20), their combination is a logical choice. Hence, a force field, termed ff99SBnmr1-ILDN, incorporating the ff99SBnmr1 backbone torsion potential and the ff99SB-ILDN side-chain torsion potential is employed in this work to explore ubiquitin side-chain motions up to the microsecond timescale.

Generally, protein side chains can undergo motions on timescales much slower than the ps-ns motions probed by spin relaxation. Therefore, NMR parameters that are sensitive to those timescales can play an invaluable role in understanding slower side-chain motions into the ns, μs, and even ms range. Residual dipolar couplings (RDCs), which probe motions up to the millisecond timescale, are uniquely suited for this purpose (21–23). Recently, Farès et al. (24) applied the model-free approach (22) to analyze the methyl group RDCs in ubiquitin and revealed the existence of substantial

Submitted April 6, 2011, and accepted for publication June 29, 2011.

*Correspondence: bruschweiler@magnet.fsu.edu

Editor: Patrick Loria.

0006-3495/11/08/0910/6 $2.00

doi: 10.1016/j.bpj.2011.06.053

side-chain motions in the supra-τ_c time window. For the purpose of validating MD trajectories, a large set of experimental couplings preferably measured in multiple alignment media are required due to the degeneracy of bond orientations in RDC values. For human ubiquitin, methyl group RDCs measured in different alignment media have been reported by different labs (21,24,25). In the current work, we employ this large body of methyl group RDC data for an objective and unobstructed assessment of a microsecond MD trajectory. It is found that the slow side-chain motions can be increasingly accurately predicted by the latest generation of molecular mechanics force fields.

METHODS

Molecular dynamics simulation

A new version of AMBER ff99SB force field (12), ff99SBnmr1-ILDN, which incorporates the optimized backbone (19) and side-chain (20) torsion potentials, was employed for 1 μs simulation of free ubiquitin with the TIP3P explicit water model (26) using the GROMACS software package version 4.0.7 (27). The optimized side-chain force field for the four amino acids Ile, Leu, Asp, and Asn (Table 1 in (20)) was implemented in GROMACS in a tabulated form with 0.1° spacing and cubic spline interpolation. The crystal structure of ubiquitin (PDB code: 1UBQ) (28) was used as the initial conformation. The van der Waals interactions were cut off at 10 Å. The short range electrostatic interactions were cut off at 8 Å and the long-range electrostatic interactions were treated with the particle-mesh Ewald summation method (29). All bonds involving hydrogen atoms were constrained using the LINCS algorithm (30) and the integration step was set to 2 fs. Standard minimization and equilibration procedures described previously (31) were applied before the final production run under the NPT condition. The temperature during the course of the simulation was kept at 300 K with coupling constant of 0.1 ps by the velocity rescaling algorithm (32) and the pressure was kept at 1 bar with coupling constant of 2 ps with the Parrinello-Rahman barostat (33,34).

Back-calculation of methyl group RDCs

For each alignment medium an alignment tensor ($\mathbf{A}$) was determined independently of the side-chain RDC data. For this purpose, a set of backbone NH RDCs from each medium was used to fit $\mathbf{A}$ by singular value decomposition as described previously (13) and subsequently rescaled to the axial CC bond of individual methyl groups according to $\mathbf{A}_{CC} = -0.1963\mathbf{A}_{NH}$ (24). The RDC values were then calculated from the MD trajectory as $D_{calc} = \langle \mathbf{e}^T\mathbf{A}\mathbf{e}\rangle$, where $\mathbf{e}$ is an individual normalized CC bond vector, and the angular bracket denotes ensemble averaging over the snapshots of the trajectory. For comparison of experimental and back-calculated RDCs, the experimental methyl RDCs were also rescaled to the corresponding values of the axial CC bond according to $D_{CC} = -0.3155D_{CH3}$ (25).

To evaluate the dependence of Q values, as measures of consistency between experiment and simulation, on the trajectory length, $<Q_{av}>$ is calculated as

$$<Q_{av}> = \left\langle \frac{1}{N}\sum_{n=1}^{N}\left[\frac{\sqrt{\sum_{vectors}\left(RDC_{calc}-RDC_{exp}\right)^2}}{\sqrt{\sum_{vectors}RDC_{exp}^2}}\right]\right\rangle_{windows}, \quad (1)$$

where N is the number of different alignment media, and RDC_{calc} (RDC_{exp}) denote back-calculated (experimental) CC bond RDC values. The angular bracket denotes the averaging of Q_{av} values calculated from multiple time windows of the same length taken from the same 1 μs trajectory, and the number of time windows for each window size is determined by the total simulation time divided by the corresponding time window size.

For the purpose of force field comparison, a previously reported 1 μs MD trajectory of free ubiquitin simulated with the original ff99SB force field (16) was also used for the back-calculation of RDCs.

Back-calculation of generalized order parameters

The nontail backbone region of ubiquitin (residues 2–71) was first superimposed for the entire MD ensemble to remove overall rotational and translational motion. For each normalized axial CC bond vector $\mathbf{e} = [x\ y\ z]^T$, the order parameter was calculated as (35–37):

$$S^2 = \frac{3}{2}\left[\langle x^2\rangle^2+\langle y^2\rangle^2+\langle z^2\rangle^2+2\langle xy\rangle^2+2\langle xz\rangle^2+2\langle yz\rangle^2\right]-\frac{1}{2}, \quad (2)$$

where angular brackets denote ensemble average over the 1 μs MD trajectory. The back-calculated order parameter is subsequently compared with the model-free derived RDC order parameter (24).

RESULTS AND DISCUSSION

Residue-specific agreement between RDC_{exp} and RDC_{calc}

To evaluate the performance of the optimized potentials ff99SBnmr1-ILDN, the methyl group RDCs were back-calculated from both the 1 μs MD trajectory and the EROS ensemble followed by comparison with the experimental data in a residue-specific manner, as shown in Fig. 1. The EROS ensemble (21), which was specially refined against the experimental methyl RDC data in addition to other NMR observables, serves here as a useful benchmark representing an estimate for the optimal agreement one can expect between a conformational ensemble and experiment. Quite remarkably, the entirely unconstrained MD ensemble with ff99SBnmr1-ILDN is found to show an overall similar performance as the EROS ensemble (Fig. 1). Several RDC_{calc} values significantly deviate from the RDC_{exp} values for both EROS and MD ensembles, which include Cγ2 of Val-26 in alignment medium #7 and Cγ2 of Thr-7, Cδ1 of Leu-43, and Cβ of Ala-28 in alignment medium #11. Two of these RDCs (Thr-7 and Leu-43) show unusually large error bars in the experiment due to weak resonances in the spectrum. A moderately better performance of Leu residues is seen in EROS than the MD ensemble; however, the performance of Leu in both MD and EROS ensembles is clearly poorer than for the other methyl-bearing residue types. The RDCs of Val and Ala methyls are also slightly better reproduced by EROS than MD. For Ala, the slope RDC_{exp}/RDC_{calc} of the EROS ensemble is slightly closer to one than for the MD ensemble (Fig. 1). However, because there are only two Ala residues in ubiquitin it is not clear whether

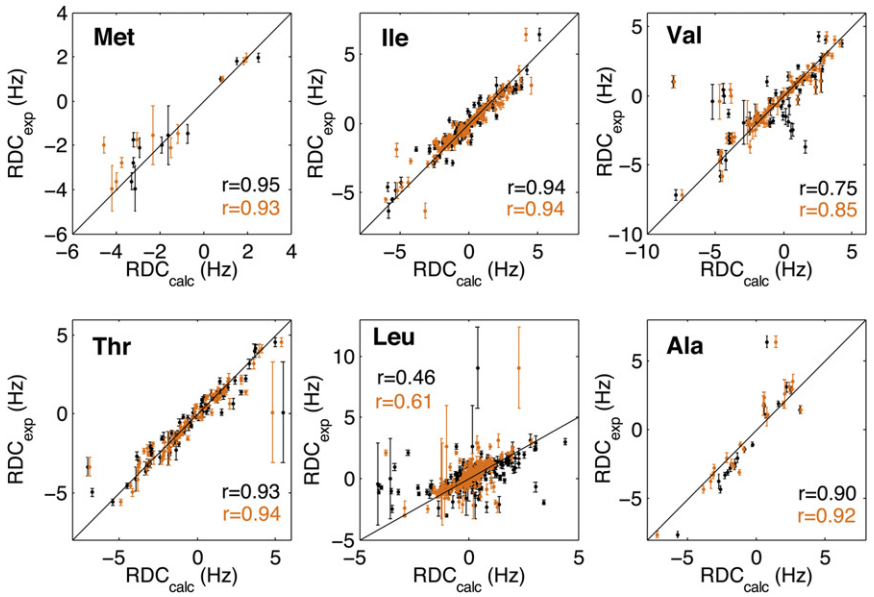

FIGURE 1 Methyl side-chain RDC_{calc} values derived from a 1 μs MD trajectory of ubiquitin with the ff99SBnmr1-ILDN force field (*black*) and the EROS ensemble (*orange*) (21) versus the corresponding experimental RDC_{exp} values for six individual methyl-containing residue types. When the Leu-43 Cδ1 outlier (RDC_{exp} = 9.05 Hz) is excluded, the correlation coefficient r for the leucine RDCs increases to 0.53 (0.62) for the MD (EROS) ensemble.

this is an Ala-specific property. Interestingly, a recent MD trajectory (using ff99SB) has shown good agreement with experimentally determined Cα-Hα relaxation order parameters (S^2) (38), which for the most part sense the same types of sub-ns backbone motions as the Cα-Cβ vectors (39). Still, the present result attests to the high quality of ff99SBnmr1-ILDN and shows a promising trend to predictively understand the slow motions of protein side chains with the latest generation of force fields, absent of any guidance by experimental restraints.

Improvement of ff99SBnmr1-ILDN over the original ff99SB

For the purpose of force field comparison, the RDCs were also back-calculated from the ensemble calculated with the original ff99SB force field, followed by comparison with the ff99SBnmr1-ILDN force field. To estimate the statistical errors of RDC_{calc}, the full trajectory was divided into three parts (0.33 μs each), followed by back-calculation of RDCs for each part. The statistical errors were estimated based on the standard deviations of the individually back-calculated RDCs, and the corresponding mean values were subsequently compared to the experimental data (Fig. 2). Additional comparisons of the performance of ff99SB, ff99SBnmr1, and ff99SBnmr1-ILDN are provided in Fig. S1 in the Supporting Material.

Notably, the χ_1 potential of Ile, which has been optimized in the force field ff99SBnmr1-ILDN, significantly improves the agreement between simulation and experiment, with the correlation coefficient (r) increasing from 0.80 (ff99SB) to 0.94 (ff99SBnmr1-ILDN). Some improvement is also found for Leu with the correlation coefficient r increasing from 0.35 to 0.46. However, the statistical errors of RDC_{calc} for Leu, which are noticeably larger than for other residue types, show that for this residue type convergence has not been achieved over the 1 μs duration of the simulation. For Ile, the improvement of the optimized potential substantially exceeds the relatively small statistical errors, demonstrating a statistically improved overall performance of ff99SBnmr1-ILDN over ff99SB.

Convergence of RDC *Q* values as a function of trajectory length

Experimentally determined RDC values are motionally averaged parameters sensitive to slow dynamics up to the millisecond timescale. To test the convergence of the present simulation as well as to illuminate the motional timescales behind these NMR parameters in ubiquitin, the dependence of $<Q_{av}>$ on the length of the time window is computed, as shown in Fig. 3. The $<Q_{av}>$ values rapidly drop with the increase of the trajectory length from 0.1 ns to 1 μs reflecting the absence of fully converged $<Q_{av}>$ for most residues. Met is the only exception reaching a plateau after ~10 ns. Presumably, this is because the only Met residue in ubiquitin is the first amino acid in the ubiquitin sequence, M1, whose side chain samples conformational space more freely and more rapidly than most other side chains.

Fig. 3 also shows the distinctive behavior of Leu from all other methyl-containing residues. The initial value $<Q_{av}>(t = 0.1$ ns) of Leu is exceptionally high, which indicates that in the experiment the Leu side chains tend to sample a wider range of conformational substates, including different rotameric states, and its RDC values cannot be accurately accounted for by the fast motions probed during the MD simulation. Although $<Q_{av}>(t = 1$ μs) of Leu remains the highest among all six residue types, which is

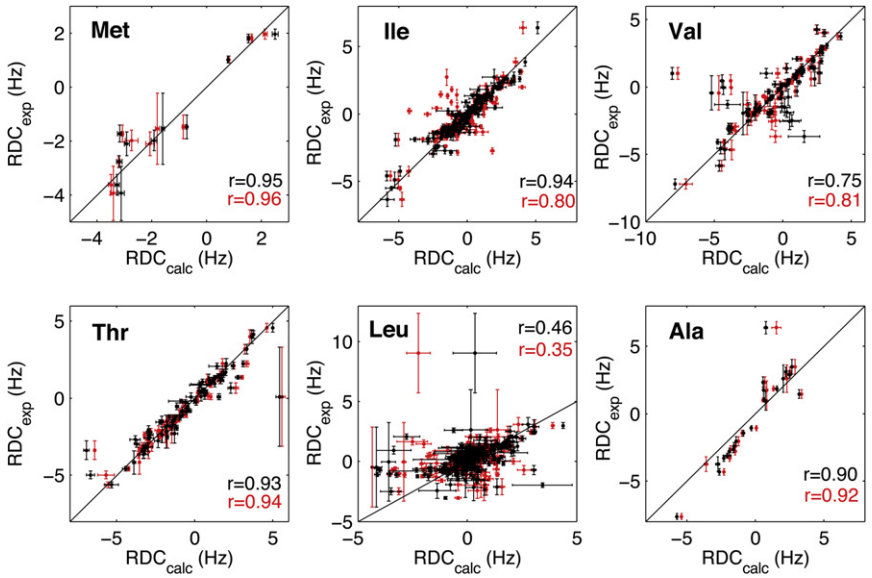

FIGURE 2 Methyl side-chain RDC_{calc} values calculated from the MD trajectories using ff99SB (*red*) and ff99SBnmr1-ILDN (*black*) versus the corresponding experimental RDC_{exp} values for six individual methyl-containing residue types. The statistical errors of RDC_{calc} are estimated based on the standard deviations of three subtrajectories of 0.33 μs length each.

mirrored in the scatter plots of Figs. 1 and 2, the improvement of agreement for Leu is the largest ($\Delta<Q_{av}> = 0.6$) when the time window increases from 0.1 ns to 1 μs. However, based on convergence tests, we anticipate that there are additional conformations that have not been sufficiently explored by the current simulation.

Axial order parameters of methyl groups

The generalized order parameters of individual CH_3 groups are back-calculated from the 1 μs trajectory (S^2_{MD}), and compared with the ones (24) derived from RDC-based model-free analysis (S^2_{RDC}) (Fig. 4). Since the present simulation time does not cover the full range of timescales (ps–ms) to which experimental RDCs are sensitive to, the following inequality is expected to hold: $S^2_{MD} \geq S^2_{RDC}$. Indeed, it is found that S^2_{RDC} is systematically lower than S^2_{MD} (Fig. 4), largely independent of residue types and locations. This result agrees with the slow nature of these side-chain motions, consistent with the convergence test shown above. Side-chain motions that exceed the microsecond time scale may also contribute to transverse spin relaxation rates via exchange contributions, which can be tested in future experimental studies.

CONCLUSIONS

The recent modification of side-chain torsion potentials for four amino acids (Ile, Leu, Asp, and Asn) opened a promising prospect of predicting side-chain motions with higher

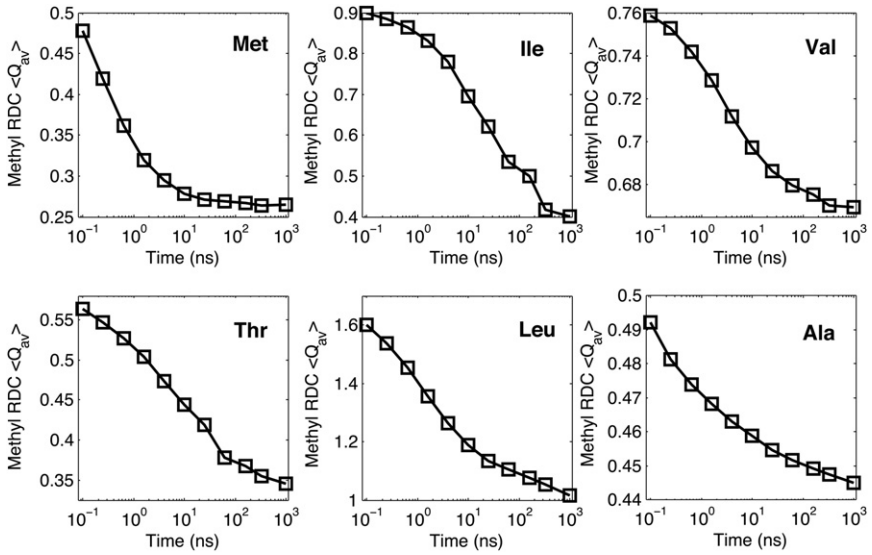

FIGURE 3 Dependence of methyl RDC $< Q_{av} >$ values on the time window size from 0.1 ns to 1 μs for the six methyl-containing amino-acid residue types. The trajectory used was computed with the force field ff99SBnmr1-ILDN.

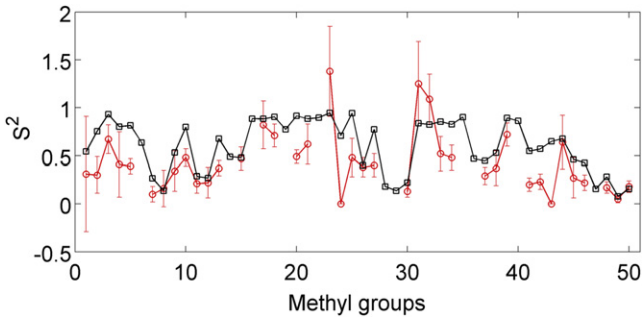

FIGURE 4 Axial C-CH_3 order parameters (S^2) of individual methyl groups derived from a model-free analysis of experimental RDCs (*red open circle*) (24) and back-calculated from a 1 μs MD trajectory with the force field ff99SBnmr1-ILDN (*black open square*). Table S1 serves as a lookup table between methyl group numbers (x axis) and the amino acid identities.

accuracy and reliability. In this study, we incorporate these modified side-chain potentials into ff99SBnmr1, a modified version of ff99SB with improved backbone potentials, and used this new force field, ff99SBnmr1-ILDN, to explore the ubiquitin side-chain motions up to 1 μs for direct comparison with experimental methyl group RDC data. The result reveals a high level of consistency between back-calculated and experimental RDC values for five of the six residue types (Met, Ile, Val, Thr, and Ala), and shows a moderate improvement of ff99SBnmr1-ILDN over the original ff99SB as confirmed by statistical analysis. Remarkably, the free simulation in the absence of any experimental restraints predicts the side-chain slow motions on a similar level of accuracy as the specifically refined EROS ensemble. These results suggest that the conformational dynamics of side chains involved in various physiologically critical processes can be realistically studied on a wide range of timescales by MD simulations using ff99SBnmr1-ILDN. In addition, the modified side-chain potentials also improve the backbone motions of ubiquitin (Fig. S1), which corroborates the interdependence of side-chain dynamics and backbone dynamics observed previously (15). The remaining discrepancy between experiment and simulation can at least be partially attributed to slower side-chain dynamics that are reflected in the RDCs, but are not adequately sampled during the course of the present trajectory, as is evidenced by direct comparison between order parameters derived from simulation and experiment. This realization is important for future force field validation and optimization efforts as well as in silico studies on the atomic details of the functional roles of side chains in a wide range of biomolecular processes.

SUPPORTING MATERIAL

Two tables, five figures, and references are available at http://www.biophysj.org/biophysj/supplemental/S0006-3495(11)00783-1.

This work was supported by grant MCB-0918362 from the National Science Foundation (to R.B.) and the Max Planck Society, the Fonds der Chemischen Industrie, the German Israel Funds, the Deutsche Forschungsgemienschaft and the European Research Council (grant agreement No. 233227) (to C.G.).

REFERENCES

1. Boehr, D. D., R. Nussinov, and P. E. Wright. 2009. The role of dynamic conformational ensembles in biomolecular recognition. *Nat. Chem. Biol.* 5:789–796.
2. Henzler-Wildman, K., and D. Kern. 2007. Dynamic personalities of proteins. *Nature.* 450:964–972.
3. Lee, A. L., and A. J. Wand. 2001. Microscopic origins of entropy, heat capacity and the glass transition in proteins. *Nature.* 411:501–504.
4. Choy, W. Y., D. Shortle, and L. E. Kay. 2003. Side chain dynamics in unfolded protein states: an NMR based 2H spin relaxation study of delta131delta. *J. Am. Chem. Soc.* 125:1748–1758.
5. Kay, L. E., D. R. Muhandiram, …, J. D. Forman-Kay. 1998. Correlation between binding and dynamics at SH2 domain interfaces. *Nat. Struct. Biol.* 5:156–163.
6. Lee, A. L., S. A. Kinnear, and A. J. Wand. 2000. Redistribution and loss of side chain entropy upon formation of a calmodulin-peptide complex. *Nat. Struct. Biol.* 7:72–77.
7. Tugarinov, V., and L. E. Kay. 2005. Methyl groups as probes of structure and dynamics in NMR studies of high-molecular-weight proteins. *ChemBioChem.* 6:1567–1577.
8. Ruschak, A. M., and L. E. Kay. 2010. Methyl groups as probes of supra-molecular structure, dynamics and function. *J. Biomol. NMR.* 46:75–87.
9. Esadze, A., D.-W. Li, …, J. Iwahara. 2011. Dynamics of lysine side-chain amino groups in a protein studied by heteronuclear 1H−15N NMR spectroscopy. *J. Am. Chem. Soc.* 133:909–919.
10. Otten, R., J. Villali, …, F. A. Mulder. 2010. Probing microsecond time scale dynamics in proteins by methyl (1)H Carr-Purcell-Meiboom-Gill relaxation dispersion NMR measurements. Application to activation of the signaling protein NtrC(r). *J. Am. Chem. Soc.* 132:17004–17014.
11. Marlow, M. S., J. Dogan, …, A. J. Wand. 2010. The role of conformational entropy in molecular recognition by calmodulin. *Nat. Chem. Biol.* 6:352–358.
12. Hornak, V., R. Abel, …, C. Simmerling. 2006. Comparison of multiple Amber force fields and development of improved protein backbone parameters. *Proteins.* 65:712–725.
13. Showalter, S. A., and R. Brüschweiler. 2007. Quantitative molecular ensemble interpretation of NMR dipolar couplings without restraints. *J. Am. Chem. Soc.* 129:4158–4159.
14. Showalter, S. A., and R. Brüschweiler. 2007. Validation of molecular dynamics simulations of biomolecules using NMR spin relaxation as benchmarks: application to the AMBER99SB force field. *J. Chem. Theory Comput.* 3:961–975.
15. Showalter, S. A., E. Johnson, …, R. Brüschweiler. 2007. Toward quantitative interpretation of methyl side-chain dynamics from NMR by molecular dynamics simulations. *J. Am. Chem. Soc.* 129:14146–14147.
16. Li, D.-W., and R. Brüschweiler. 2010. Certification of molecular dynamics trajectories with NMR chemical shifts. *J. Phys. Chem. Lett.* 1:246–248.
17. Wickstrom, L., A. Okur, and C. Simmerling. 2009. Evaluating the performance of the ff99SB force field based on NMR scalar coupling data. *Biophys. J.* 97:853–856.
18. Cerutti, D. S., P. L. Freddolino, …, D. A. Case. 2010. Simulations of a protein crystal with a high resolution x-ray structure: evaluation of force fields and water models. *J. Phys. Chem. B.* 114:12811–12824.
19. Li, D.-W., and R. Brüschweiler. 2010. NMR-based protein potentials. *Angew. Chem. Int. Ed. Engl.* 49:6778–6780.
20. Lindorff-Larsen, K., S. Piana, …, D. E. Shaw. 2010. Improved side-chain torsion potentials for the Amber ff99SB protein force field. *Proteins.* 78:1950–1958.

21. Lange, O. F., N.-A. Lakomek, …, B. L. de Groot. 2008. Recognition dynamics up to microseconds revealed from an RDC-derived ubiquitin ensemble in solution. *Science.* 320:1471–1475.

22. Meiler, J., J. J. Prompers, …, R. Brüschweiler. 2001. Model-free approach to the dynamic interpretation of residual dipolar couplings in globular proteins. *J. Am. Chem. Soc.* 123:6098–6107.

23. Tolman, J. R. 2002. A novel approach to the retrieval of structural and dynamic information from residual dipolar couplings using several oriented media in biomolecular NMR spectroscopy. *J. Am. Chem. Soc.* 124:12020–12030.

24. Farès, C., N.-A. Lakomek, …, C. Griesinger. 2009. Accessing ns-micros side chain dynamics in ubiquitin with methyl RDCs. *J. Biomol. NMR.* 45:23–44.

25. Ottiger, M., and A. Bax. 1999. How tetrahedral are methyl groups in proteins? A liquid crystal NMR study. *J. Am. Chem. Soc.* 121:4690–4695.

26. Jorgensen, W. L., J. Chandrasekhar, …, M. L. Klein. 1983. Comparison of simple potential functions for simulating liquid water. *J. Chem. Phys.* 79:926–935.

27. Van Der Spoel, D., E. Lindahl, …, H. J. Berendsen. 2005. GROMACS: fast, flexible, and free. *J. Comput. Chem.* 26:1701–1718.

28. Vijay-Kumar, S., C. E. Bugg, and W. J. Cook. 1987. Structure of ubiquitin refined at 1.8 A resolution. *J. Mol. Biol.* 194:531–544.

29. Darden, T., D. York, and L. Pedersen. 1993. Particle mesh Ewald: an *N*-log(*N*) method for Ewald sums in large systems. *J. Chem. Phys.* 98:10089–10092.

30. Hess, B., S. Becker, …, J. G. E. M. Fraaije. 1997. LINCS: a linear constraint solver for molecular simulations. *J. Comput. Chem.* 18:1463–1472.

31. Long, D., and R. Brüschweiler. 2011. In silico elucidation of the recognition dynamics of ubiquitin. *PLoS Comput. Biol.* 7:e1002035.

32. Bussi, G., D. Donadio, and M. Parrinello. 2007. Canonical sampling through velocity rescaling. *J. Chem. Phys.* 126:014101.

33. Parrinello, M., and A. Rahman. 1981. Polymorphic transitions in single crystals: a new molecular dynamics method. *J. Appl. Phys.* 52:7182–7190.

34. Nose, S., and M. L. Klein. 1983. Constant pressure molecular dynamics for molecular systems. *Mol. Phys.* 50:1055–1076.

35. Chatfield, D. C., A. Szabo, and B. R. Brooks. 1998. Molecular dynamics of *Staphylococcal nuclease*: comparison of simulation with 15N and 13C NMR relaxation data. *J. Am. Chem. Soc.* 120:5301–5311.

36. Hu, H., M. W. Clarkson, …, A. L. Lee. 2003. Increased rigidity of eglin c at acidic pH: evidence from NMR spin relaxation and MD simulations. *Biochemistry.* 42:13856–13868.

37. Friedland, G. D., N.-A. Lakomek, …, T. Kortemme. 2009. A correspondence between solution-state dynamics of an individual protein and the sequence and conformational diversity of its family. *PLoS Comput. Biol.* 5:e1000393.

38. Sheppard, D., D.-W. Li, …, V. Tugarinov. 2009. Deuterium spin probes of backbone order in proteins: 2H NMR relaxation study of deuterated carbon alpha sites. *J. Am. Chem. Soc.* 131:15853–15865.

39. Brüschweiler, R. 1995. Collective protein dynamics and nuclear spin relaxation. *J. Chem. Phys.* 102:3396–3403.